

EFFECT OF DIATOMACEOUS EARTH ON DESICCATION CRACKING OF EXPANSIVE SOILS

*Alemshet Bekele Tadesse¹, Yoshinori Fukubayashi², Atsushi Koyama³, and Daisuke Suetsugu³

¹ Interdisciplinary Graduate School of Agri. and Eng., University of Miyazaki, Japan

^{2,3} Faculty of Engineering, University of Miyazaki, Japan

*Corresponding Author, Received: 15 Dec. 2022, Revised: 09 Jan. 2023, Accepted: 31 Jan 2023

ABSTRACT: Expansive soils shrink and swell, causing considerable density differences as the moisture content varies and cracks develop as the soil dries. This cracking condition has a detrimental effect on the stability of infrastructure built on expansive soil, such as road embankments. This paper investigates the influence of diatomaceous earth (at 5%, 10%, 15%, and 20% DE percent by mass) on the desiccation cracking of expansive soils. The report demonstrates an image analysis technique to describe soil surface cracking quantitatively. The geometric features of cracks, such as surface crack area and crack connectivity, were estimated and examined. The study considers soil crack area ratio and cracking index to investigate the effect of diatomaceous earth on expansive soil surface cracking. The crack area ratio and cracking index analysis results show that the expansive soil surface cracking is uneven and significant. The soil matrix containing 10% and 20% diatomaceous earth has reduced surface cracking and a homogenous radial cracking pattern. The image analysis approach, an essential method to quantitatively quantify soil desiccation cracking, revealed that diatomaceous earth substantially affects surface crack reduction.

Keywords: Expansive Soil, Desiccation Cracking, Diatomaceous Earth (DE), Image Analysis

1. INTRODUCTION

Shrinkage and swelling of expansive soil are commonly observed physical phenomena in civil engineering applications, primarily due to the dynamic change of soil pore structure at a micro level and macroscopically manifested in volume change response to moisture variation in the wet and dry season [1, 2]. In the dry season, desiccation cracking develops arising from water loss. These desiccation cracks are more common in tropical countries such as Ethiopia due to the prevalent occurrence of expansive soils (i.e., vertisols account for around 10% of the total soil distribution in Ethiopia), as illustrated in Fig. 1 below, which is the soil distribution map of Ethiopia.

This phenomenon covers a wide variety of scales, from a fraction of smaller sizes to larger scale sizes. As a result, soil desiccation cracking is receiving extensive attention in geotechnical engineering and other related disciplines [3]. Desiccation cracks illustrated in Fig. 2 are caused mainly by shrinkage due to rapid water evaporation from the soil surface. These desiccation cracks induce an interparticle tension and volume change, increasing cracking permeability and reducing soil stability due to the generated flow paths. It has also been noted that the temperature in Ethiopia ranges from 27°C to 50°C; due to this climatic change, rapid water evaporation occurs, leading to desiccation crack [4].

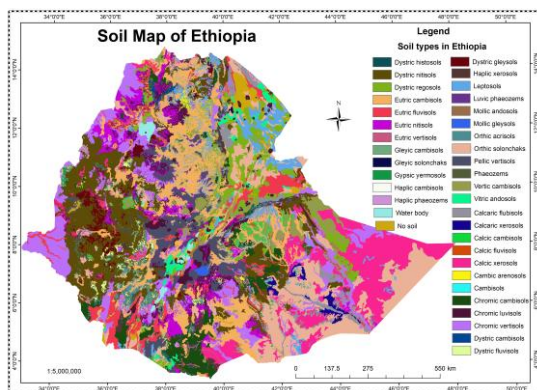


Fig. 1 Soil Map of Ethiopia



Fig. 2 Desiccation cracking in expansive natural soil (Source: <http://geophilous.blogspot.com>)

In general, rainfall assists in the partial or complete self-recovery of cracks during the wet season, as shown in Fig. 3 on the surface in shallow and narrower cracks, whereas heavy rainfall in combination with hot weather contributes to desiccation cracking. The resulting formation of cracking networks negatively alters the soil properties and compromises the integrity of soil structures [5].

The mechanical properties of soils subjected to desiccation cracking are affected by increased compressibility, excessive deformation, and weakened strength. The ultimate reduction of performance and failure of civil infrastructures are due to the combined effects of desiccation cracking influence parameters [6]. A critical influence on the performance of geotechnical engineering structures such as road embankments occurs due to desiccation cracking dictating remedial or eradication solutions such as altering soil property and providing a moisture barrier [7].

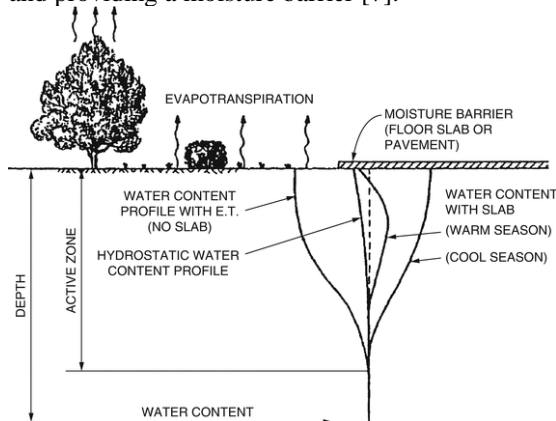


Fig. 3 Water content profiles in active zones[8]

Different researchers investigate mitigating desiccation cracking by the influence of additives such as cement, lime, sand, fibers, and bio-enzymes [5, 9]. These studies focused on hydraulic conductivity and volumetric shrinkage of clay soil. Where these additives can reduce shrinkage but sometimes increment in permeability might be observed. Ahmed F. et al. (2021) [10] also studied the polypropylene fiber effect on desiccation cracking under multiple wetting-drying cycles on kaolinite clay, and the reinforcement reduces cracking.

Very recently, Yaxing et al. (2021) [9] studied the use of fibers (i.e., jute fiber and polyvinyl alcohol fiber (PVA)) and illustrated the evolution of desiccation cracking by applying the digital image correlation (DIC) method. These experimental results showed that the presence of fibers significantly affects the crack evolution and the reinforced soil's length and area during shrinkage.

Furthermore, many other studies have also been conducted on reducing desiccation cracking by utilizing multiple additives in fiber or chemicals to

improve shrinkage limits, tensile strength, shear strength, and hydraulic conductivity. However, adding those additives does not significantly affect the mechanical behavior of clay soils. Hence, further investigations are required to understand, quantitatively analyze, and express treated soils comprehensively. Besides, very few studies have been conducted on the effect of diatomaceous earth (DE) on the desiccation cracking reduction of expansive soils. Diatomaceous earth is preferred in this study due to its rich silica content (SiO_2). It was hypothetically assumed that the silica and other chemical elements in the additive would remove and replace the water molecules of the expansive clay surface and reduce shrinkage and swelling.

Thus, this study aims to study the effect of diatomaceous earth on the desiccation cracking of expansive soil by using image analysis techniques to capture the crack morphology, mode of cracking, and crack connectivity. The diatomaceous earth is mixed at 5%, 10%, 15%, and 20% by mass, and the desiccation cracking experimental parameters were examined during drying.

2. RESEARCH SIGNIFICANCE

Through thoroughly assessing this study on desiccation cracking, the effect of diatomaceous earth on desiccation cracking is observed. Moreover, this research will clarify the mechanism of desiccation cracking and cracking reduction mechanism using diatomaceous earth additives. In this regard, this study will give a clear insight into the mechanism of desiccation cracking development and reduction due to the application of the diatomaceous earth additive. Moreover, the image analysis made by this study quantitatively described the desiccation cracking. In addition to this, the overview presented in this research will move forward for new understandings, which will be helpful in the future examination of the desiccation reduction of expansive soils by using diatomaceous earth additives and might lead to more in-depth analysis.

3. MATERIALS AND METHODS

3.1 Materials

3.1.1 Expansive Soil

The materials used in this study are expansive natural soil from Yanaizu Area, Fukushima Prefecture, Japan, and designated as Yanaizu expansive soil (YES) in this study. Filter-grade diatomaceous earth is purchased from the market in Japan. The pertinent characteristics of the soil are shown in Table 1. Soil particles that pass through a $425\mu\text{m}$ sieve were subjected to the free swell index test. The result signifies that the soil is a very high

expansive soil per IS 2720-40 and very high inorganic clayey soil according to ASTM D2487 universal soil classification system. The chemical composition of materials from the energy dispersive spectrometry (EDAX) test is presented in Table 2 below of the expansive soil of Japan.

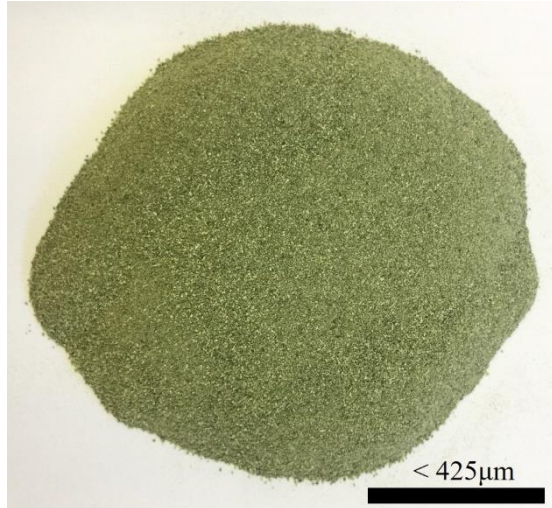


Fig. 4 Yanaizu Expansive Soil (YES)

Table 1 Physical Properties of Yanaizu expansive soil

Soil Property		Value	Standard
Liquid Limit, LL (%)		134.3	ASTM D4318
Plastic Limit, PL (%)		42.3	
Plastic Index, PI (%)		92	
Color		Green	
Particle Size Distribution	Gravel (%)	13.5	JGS0131
	Sand (%)	32.2	
	Silt (%)	0.3	
	Clay (%)	54	
Free Swell Index, FSI (%)		134	IS 2720-40
Specific Gravity (ρ_s , g/cm ³)		2.55	JGS0111
Soil Class	USCS	CH	ASTM D2487
	AASHTO	Clay	AASHTOM145

AASHTO: American Association of Highway & Transport Office
 ASTM: American Standard Testing Method
 IS.: Indian Standard; USCS.: Universal Soil Classification System

Table 2 Chemical Composition of Materials

Chemical Composition (Oxides)	Value, %	
	YES	DE
SiO ₂	72.88	90.33
Al ₂ O ₃	14.86	5.97
Fe ₂ O ₃	5.98	2.5
CaO	-	0.69
MgO	2.55	0.25
K ₂ O	2.4	0.26
Na ₂ O	1.33	1.26

Where: YES: Yanaizu Expansive Soil
 DE: Diatomaceous Earth

3.1.2 Diatomaceous Earth

Filter-grade diatomaceous earth was used as an additive in experimental desiccation tests. The initial idea of the study was to utilize brewery silage diatomaceous obtained from beer filtration waste. However, it is not easily obtained in Japan; so, instead commercially available filter grade DE was purchased from the Showa Chemical Industry Co., Ltd of Japan. Diatomaceous earth was preferred because of its rich silica content (see Table 2) with a hypothesis that the cations of the soil minerals will be replaced by the cations of DE Si, or Al, Fe, and Ca cations due to cation exchange phenomena [11]. Those ion exchanges possibly will influence the capillary suction and tensile strength and later reflect on desiccation cracking reduction.

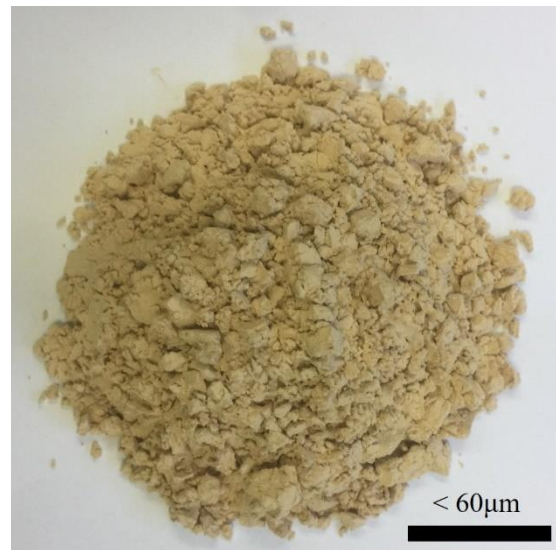


Fig. 5 Diatomaceous Earth (DE)

3.2 Methods

3.2.1 Mix Design and Sample Preparation

This study examined five mix designs of one control (natural soil) which passes through a 425 μ m sieve, and four diatomaceous earth-soil treated blends, as shown in Table 3 below. Therefore, the soil matrix designation coding system herein, shown in Table 3, is adopted.

Table 3 Soil mix design of the experiment

Mix Group	Designation	DE, %
Control ¹	ES + 0%DE	0
	ES + 05%DE	5
DE Treated	ES + 10%DE	10
	ES + 15%DE	15
	ES + 20%DE	20

¹Yanaizu Expansive Soil, DE: Diatomaceous Earth
 The diatomaceous earth and water content percent

are determined using Eq. (1) and Eq. (2) according to the phase diagram illustrated in Fig. 6 below.

$$\%DE = \frac{m_{DE}}{m_{ES}} \times 100, \quad (1)$$

$$\%\omega_c = \frac{m_w}{m_{DE} + m_{ES}} \times 100, \quad (2)$$

where DE= DE content; ω_c = water content; m_{DE} = mass of DE; m_{ES} = mass of expansive soil solids, and m_w = mass of water.

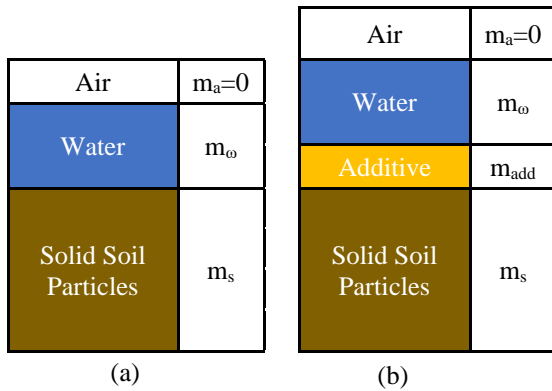


Fig. 6 Phase diagram for (a) Untreated and (b) Treated Soil Specimens

Sample preparation was done from the collected natural soil and was carefully crushed, air-dried, and sieved through a 2mm and 425 μ m sieve. Next, the saturated slurry samples were prepared by thoroughly mixing the expansive soil and diatomaceous earth as per the mix design stipulated in Table 3. Then, distilled water close to the liquid limit (LL=134.3%) amount is added to the dry mix, and great care was taken to pulverize lumped particles while mixing and targeting the homogeneity of mixtures. The slurry was then poured into 92mm diameter, 17mm height, and 2mm thickness size greased glass containers and de-aired on a horizontal shaking plate to remove the air bubbles and ensure complete saturation. Then, the slurry was sealed by a plastic cover and kept for 24 hours to have a homogenous water distribution before the desiccation experiment started.

3.2.2 Desiccation Cracking Drying Test

The desiccation cracking experiments were carried out on five saturated slurry state specimens in the laboratory. The sample was desiccated in the laboratory at a room temperature of 25 \pm 2 $^{\circ}$ C and relative humidity of 70% \pm 5% in warm environmental conditions from 3rd to 13th of Oct, 2021G.C. Digital images were taken at 135mm height above the soil sample and their respective soil mass was measured every 24hr. The experiment lasted 12 drying days, and stabilized mass and

cracked morphology were observed. Obtained cracked images were analyzed using an open-source digital image analysis tool called Fiji (ImageJ).

3.2.3 Image-Based Crack Analysis

This study presents the two-dimensional surface cracking network appearance in soil specimens tested in the laboratory. First, the digital images taken every 24hr were preprocessed by converting the color RGB Image to a calibrated grayscale image and then to a binarized and skeletonized black-and-white Image[12]. Then, the preprocessed digital images were analyzed to quantify the indication parameters specified in Eq.(3) and Eq.(4).

3.4.1 Soil Crack Intensity and Index Parameter

The study utilizes desiccation crack parameters which are the soil crack intensity (D_c) and soil crack index (r) and was computed to characterize the desiccation cracking of the untreated and treated soil specimens [13]. The intensity of soil crack and cracking index are the parameters to describe the soil cracking process, and they are expressed using the linear surface areas of the formula specified in Eqs. (3) and (4) as.

$$D_c = \sum_{i=1}^n \frac{a_c}{A} * 100\%, \quad (3)$$

Where D_c is soil crack area intensity, a_c is the sum of all soil crack areas in the typical cracked soil (mm^2), and A is the total surface area of the ordinary cracked soil (mm^2).

The spatial variation of the soil crack's morphological property is expressed in terms of connectivity which is the connection between crack topologies. Cracking index r is a ratio of crack connectivity in desiccation cracking of expansive soils. Mathematically the ratio of the corresponding crack number, the maximum possible number of connected cracks, was applied to determine the crack connectivity index expressed in Eq.(4).

$$r = \frac{L}{L_m} = \frac{L}{3(v-2)}, \quad (4)$$

Where r is the connectivity index, L is the number of connected cracks, L_m is the maximum possible interconnected cracks, and v is the number of crack nodes. The cracking index r ranges from 0 to 1, and 1 indicates higher crack connectivity.

The characterization method considers the mode of cracking observed from the untreated and treated soil specimens. Among the soil specimens tested, two specific cases were observed; the first one is irregularly desiccated samples in

diatomaceous earth treated soil matrices (i.e., YES+0%DE, YES+5%DE, and YES+15%DE), and a regular uniform radial cracking was observed in (i.e., YES+10%DE and YES+20%DE). The two cases where the irregular cracking and normal radial shrinkage are exemplified schematically are shown in Fig. 7 (a) and (b), respectively.

Fig. 7 presents the designation for the spatial distribution of surface desiccation cracking area and cracking parameters utilized using the image analysis technique. The crack area denotation described here is for two categories depending on cracking modes (see Fig. 7 a. irregular mode of cracking and b. for uniform radial desiccation cracking). The shrunk (clod) area is the final area of the soil shrink part, while cracking in between the clod areas is designated as the cracked part. The second mode has two crack area parts, the shrunk area and the uniform cracked part designated as shrunk part. In addition, the crack connectivity and index parameters are illustrated in the irregular cracking mode. The crack segment which connects the nodes (i.e., crack intersection point) is labeled as a crack.

Crack networks on the surface of soil specimens are highly irregular and difficult to measure with a manual measurement technique using a ruler or other conventional methods, which causes an error. Mistakes can be reduced with the digital image analysis method, and reliable, realistic data can be obtained. The image analysis technique is currently utilized by various studies to characterize desiccation cracking study of untreated and treated expansive soils quantitatively [13]. First, color images of the cracked samples are converted into calibrated greyscale images and later changed into binary black-and-white photos. Next, through proper engineering judgment, identify the refinement of the cracks and shrunk areas. Then, the images were scaled, converted to a greyscale image, binarized and skeletonized to identify the cracked part and shrunk areas, and quantified using Eq. (5) below.

$$SA = OA - \left(SP + \sum_{i=1}^n CP \right), \quad (5)$$

Where SA is the shrunk (clods) area; OA is the initial original uncracked area; SP is the area of the shrunk part, and CP is the area of the cracked part for the irregular cracked samples.

From the desiccation experimental result, two distinct cracking modes were observed. Irregular interconnected cracks were observed in the untreated specimen, 5% DE, and 15% DE-treated specimens. At the same time, 10% DE and 20% DE have a uniform radial shrinkage mode. The shrunk part area will be zero, and for the uniform crack, the

mode cracked part of the area in Eq. (5) will be zero.

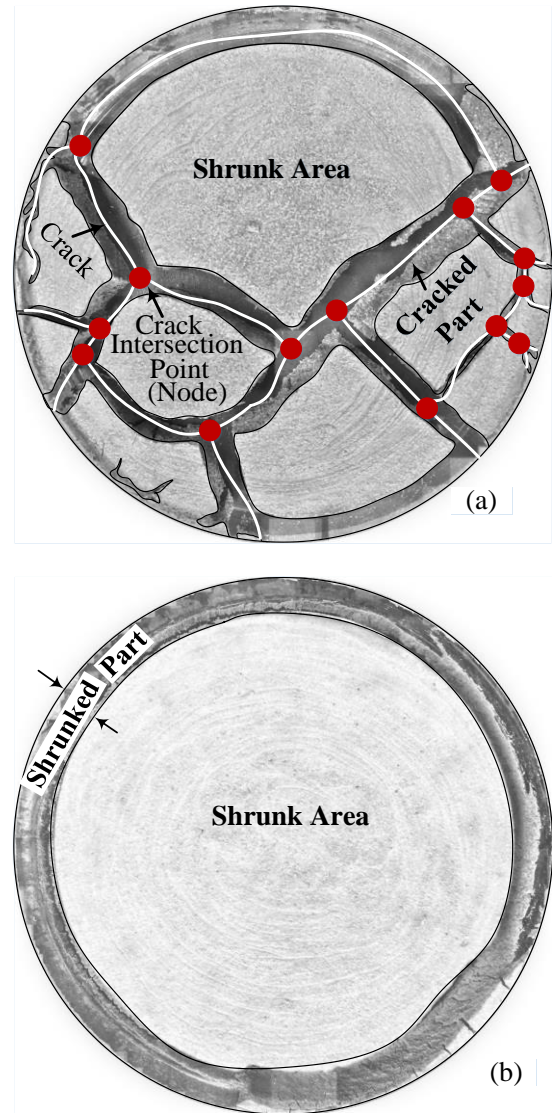


Fig. 7 Crack image processing and geometrical description of the areas (a) irregular cracking scenario and (b) uniform radial shrinkage scenario of soil specimens

4. RESULT AND DISCUSSION

4.1 Quantitative characterization of crack Area

The surface crack area ratio, crack connectivity, and cracking index parameters are considered to characterize the desiccation cracking in the soil matrices. The crack area ratio of the soil specimens is expressed in [8].

$$R_s = \frac{A_{sf}}{A_{si}}, \quad (6)$$

where R_s = Area ratio of soil specimens,
 A_{sf} = Area of the final surface area of soil specimen

after shrinkage (mm^2),

A_{si} = Area of the initial surface area of soil specimen before shrinkage (mm^2)

Fig. 8 illustrates the soil specimens' crack morphology crack area over time. The figure shows us the crack area ratio from the beginning of the crack initiation, starting from the 3rd day to the stability of cracking from the 7th to the 11th day of the desiccation cracking experiment. The crack area ratios result in the natural soil, YES+5%DE, and YES+15%DE, having effective connectivity. However, as seen in Fig. 7 (b), the soil blends YES+10%DE and YES+20%DE do not have a significant cracking index. Notably, ES+20%DE significantly reduces desiccation cracking intensity and spatial crack connectivity.

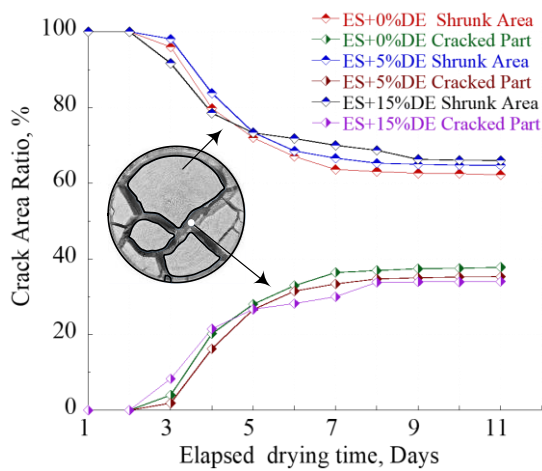


Fig. 8 Crack area ratio comparison of irregularly desiccated soil specimens

Fig 8 illustrates the cracking intensity among the soil matrices, which have irregular cracking modes. Adding 5% DE and 15% DE does not influence the desiccation cracking of the expansive soil. However, as shown in Fig. 9, the soil blends at 10%DE and 20%DE have significantly reduced crack density and connectivity morphology. Hence, desiccation cracking reduction depends on the soil mass stress state. The stress state is interdependent on different factors such as capillary suction, which in turn depends on the cation exchange capacity, tensile stress in the soil mass emanating from the suction development, and soil shear strength. Also, the cation exchange capacity depends on the carbon content, clay content, and type of minerals that needs to be studied as well.

The result in Fig. 9 presents the crack area ratio comparison among the natural soil and soil matrices at 10% and 20% diatomaceous earth-treated samples. It is observed that the DE at 10% and 20% mix has significantly reduced the desiccation cracking. The maximum crack area ratio resistance observed is at 20% DE mixture, which is about a 16% reduction from the other soil matrices.

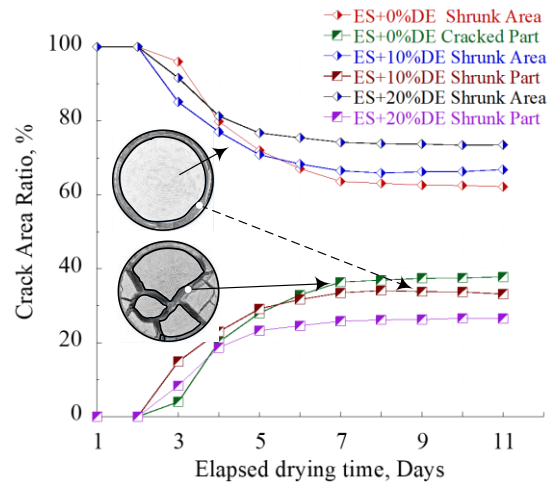


Fig. 9 Crack area ratio comparison of regularly desiccated soil specimens in a radial direction

4.2 Cracking Intensity and Cracking Index

The spatial soil crack connectivity is calculated using the connectivity index parameter r between the treated and untreated specimens. Fig. 10 and Fig. 11 illustrate the intensity of soil cracking versus diatomaceous earth content. The crack intensity (D_c) parameter decreases as the diatomaceous earth additive increases. Thus, we can depict that DE has an effect in reducing the crack density of expansive soils particularly, as we can see from Fig. 10 that the crack intensity reduces with the application of diatomaceous earth at 5% and 15% DE.

Even if the mode of cracking is similar among the untreated specimen, 5% DE and 10% DE are irregularly cracked specimens, and the experimental result implies there is about a 3% and 7% reduction in crack intensity at 5% DE and 15% DE application, respectively.

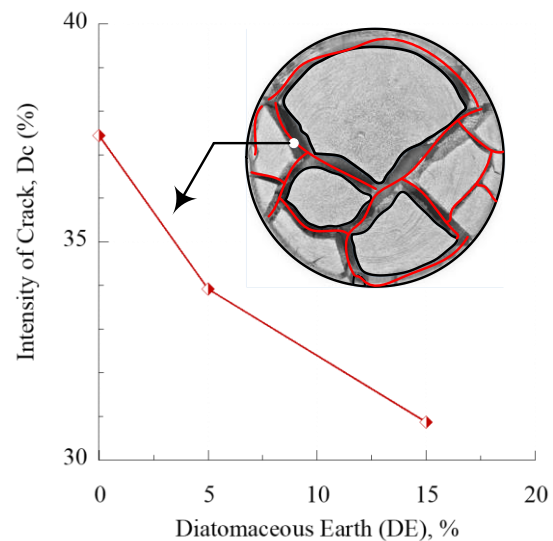


Fig. 10 Crack Intensity Comparison among the irregularly cracked specimens

Fig. 11 illustrates the crack intensity versus diatomaceous earth comparison between the cracked area of untreated soil specimens and shrunk part of uniformly radial deformed specimens at 10% and 20% DE. Notably, 6% and 11% reductions in surface clod area cracking were observed at 10% and 20% DE, respectively. Even though the trend with the application of DE showed a decrease in crack density, the mode of cracking is different among the treated specimens.

Therefore, considering the cracking mode and the quantitative experimental analysis result, we can see that surface desiccation cracking reduces as we apply diatomaceous earth (DE). Mainly, a significant reduction in the cracking mode and magnitude of the surface desiccation cracking at 10% and 20% DE application is much higher.

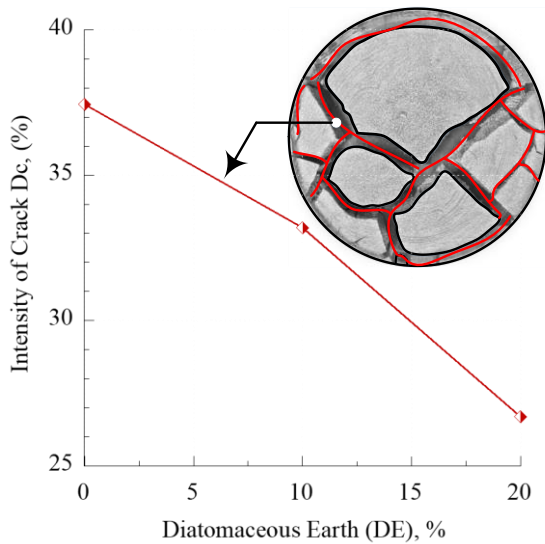


Fig. 11 Cracking intensity comparison between untreated soil, cracked part and regularly shrunk part

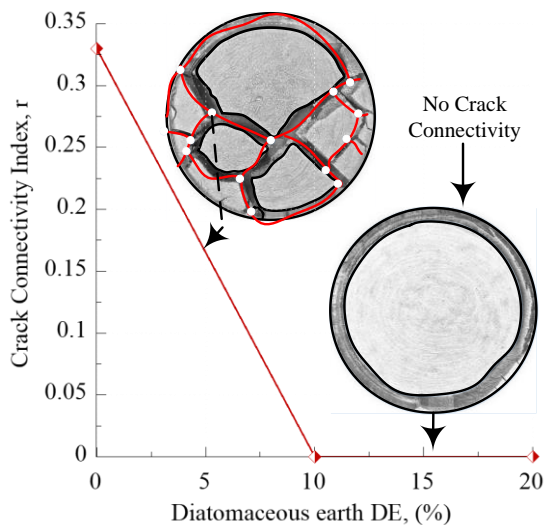


Fig. 12 Crack Connectivity Index vs. diatomaceous earth content

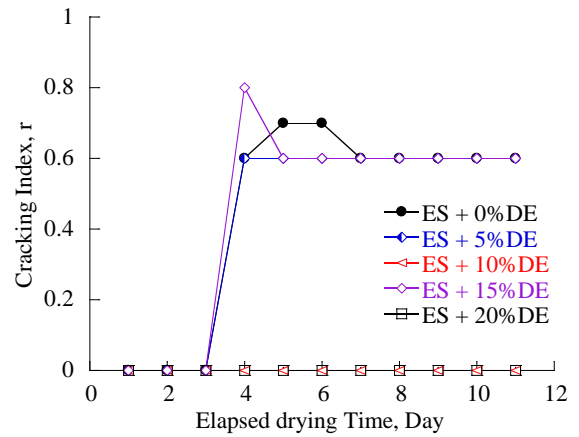


Fig. 13 Soil crack connectivity index versus elapsed time

Fig. 12 compares the crack connectivity index with the diatomaceous earth application. The result signifies no noticeable connected cracks at 10% and 20% diatomaceous earth (DE) additives. Hence, we can understand that there is a significant reduction in crack initiation and development at 10% and 20% diatomaceous earth applications.

Fig. 13 expresses the cracking index comparison over the elapsed testing days. It can be seen from Fig. 13 that Yanaizu expansive soil with 10% and 20% diatomaceous earth (DE) content has no crack connectivity. However, in the naturally expansive soil, at 5% and 15% DE content, the cracking index result ranges from 0.6 to 0.8. This cracking index results in naturally expansive soil; 5% and 15% of DE contents have shown significant interconnected cracks. Therefore, this condition has an implication for the expansive soil in terms of water permeability during wet seasons and loss of strength to bear the self-weight and external loads.

4.3 Soil water evaporation

Initially, the soil specimens have enough water in the soil pore spaces under saturated conditions. Then, during the drying state of the soil specimens, the soil water at the topmost surface of the specimen changes to water vapor and is continuously removed from the soil pores, which start from the topmost surface and get deeper [14–16]. Thus, the upward diffusion of vapor exceeds the vaporization within the soil and the vapor diffusion from the underlying layer. When the soil gets dry over the experimental dates, the evaporation rate is calculated using Eq. (7), which is adapted from reference [17]:

$$E = \frac{\Delta m}{\rho_w * A * \Delta t}, \quad (7)$$

Where E (mm/h) represents the evaporation rate, Δm (g) refers to the mass change of the tested soil

under evaporation within the time interval $\Delta t(h)$; ρ_w corresponds to the water density ($0.001g/mm^3$), and $A(mm^2)$ is the area of the magnitude of the bottom surface of the container obtained from the image analysis.

From Fig. 14, it can be observed that the evaporation rate evolution in the soil specimen under the drying desiccation experiment elapsed time and temperature difference between two consecutive days. When the desiccation drying process continues, the temperature difference increases, but on the third day of the test, the difference will drop, and crack initiation will start. Eventually, the evaporation rate decreases with the different temperatures. As it is stipulated in Fig. 14 and Table 4, the soil matrices experience a sudden evaporation rate increment at the temperature difference drop point and gradually decrease in rate, but cracks gradually develop and keep a stable crack evolution.

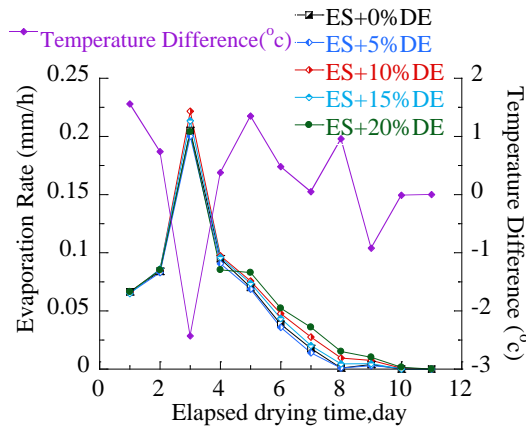


Fig. 14 Evaporation rate of tested soil specimens

4.4 Mechanism of desiccation cracking and crack reduction

4.4.1 Desiccation Cracking Mechanism

The drying test series in an open indoor laboratory atmosphere and the test results include the evolution of cracking parameters (i.e., expressed in crack area ratio, crack connectivity, and cracking index) and water evaporation rate. Fig. 16 shows the overall mechanism of desiccation cracking in clay soil. The desiccation cracking schematics illustrate and explain the gradual continuum stages of cracking and contributing factors for desiccation cracking [6]. Saturated soil specimens subjected to drying conditions experience atmospheric air contact at the specimen's top surface. Later water-vapor exchange occurs at the topmost surface, and water-air menisci happen. Eventually, at a macroscopic level, the suction value (i.e., the difference between air pressure and water pressure) at the beginning desaturation point is referred to as

the air entry value. Negative water pressure is a critical parameter in determining the desiccation property of the expansive soil when the gas phase intrudes the saturated porous soil body [18]. Hence, capillary suction in the upper layer is developed, which affects the arrangement of soil particles leading to a volume change due to the rearrangement of the soil particles.

Gradually, the subsequent process of desiccation cracking includes an interphase transfer of liquid water, and water vapor develops following several scenarios [14]. With the complexity of pore size distribution, the air intrusion is an under-surface cavity occurring in the liquid water when a constant temperature is brought to evaporation through an evolution of the suction (negative) pressure. As schematically shown in Fig. 16, water vaporizes in the soil pores and is diffused from the interior of tiny pores to a larger pore extending upwards, being exposed to the specimen's top surface. With the gradual drying of the soil specimens, the water is vaporized at deeper depths in the soil, with the vapor passing through the dry surface layer to the atmosphere, which will, in turn, affect the interparticle tensile strength[5].

Once the tensile stress is developed within the soil particles and exceeds the strength of the soil, desiccation cracks occur with the increment of suction. Also, soil microstructure usually shows heterogeneity in soil particle arrangements, even for slurry specimens signifying that the tensile bonding strength between the soil particles is not uniform [15, 19]. Under this effect of the tensile stress, the weak part of the lower bonded strength fails first; that is why more pronounced surface cracks at the top surface of the soil specimens are evolved.

Hence, at the macroscopic level, the tensile strength of the soil is critical in reflecting the soil's mechanical properties at the weakest failure zone of the soil matrix. This is further the gradual change of liquid water to vapor water and later evaporation through the soil mass macropores by diffusing from one state to another state upon drying. Finally, at the potential shrinkage state, as shown in Fig. 15, there will be remaining residual water at which the environmental temperature of the soil experiences might not remove at that experimental condition at the specified time [20].

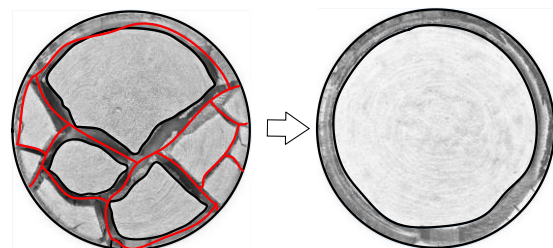


Fig. 15 Untreated specimen desiccation condition and treated specimen condition at 10% and 20% DE

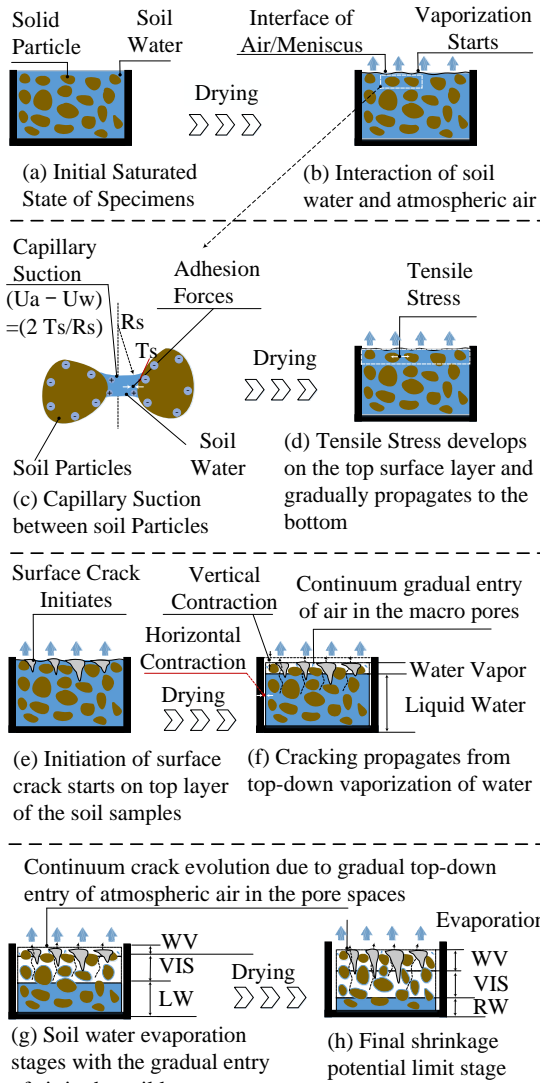


Fig. 16 Mechanism of overall soil desiccation crack schematics due to drying test
The designations shown in parts (g) and (f) of Fig. 16 are WV: water vapor, VIS: vaporization in the soil, and LW: liquid water in the soil phase change the diagrammatic description.

4.4.2 Crack Reduction Mechanism

Primary crack generation and development depend on the soil's tensile strength and the tensile stress's magnitude [5, 21]. As the significant primary cracks stabilize and secondary crack development begins, shrinkage of soil occurs, and soil particles get closer, resulting in the widening of the cracks. Fig. 17 illustrates the schematic description of the reduction in untreated and DE-treated soil specimens. Mainly, soils treated at 10%, and 20% of DE enhance the lateral and vertical shrinkage reduction, as shown in Fig. 17 below.

Moreover, the final crack area ratio for the 10% and 20% DE-treated soil has shown reduced tensile stress due to the decreased internal volumetric shrinkage of the specimens. Therefore, the effects

of diatomaceous earth on the surface desiccation crack behavior are mainly pronounced in the crack morphology with a uniform radial manner of cracking at 10% and 20% DE. However, at 0%, 5%, and 15% DE soil matrix, the specimens experience erratic desiccation cracking, and the diatomaceous earth (DE) effect is not revealed.

It has been observed that the crack networks in the natural untreated soil (ES), ES+5%DE, and ES+15%DE, experienced an irregularly desiccated crack. The propagation of the desiccation cracks in those specimens develops through a gradual further widening of the preexisting cracks until final consolidation is observed in consecutive mass measurements.

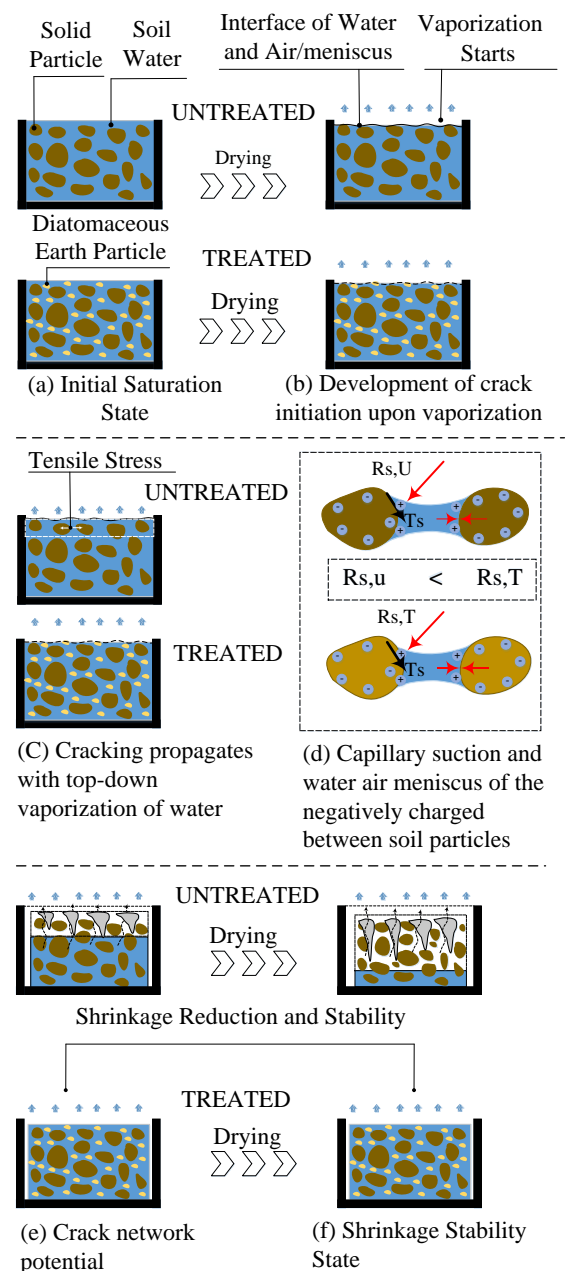


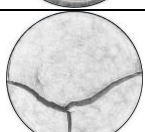
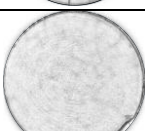
Fig. 17 Schematics of the desiccation reduction mechanism due to the application of DE additive

4.5 Cracking Initiation and End Pattern

From the observed desiccated crack images of the experimental test result, two distinct cracking modes were observed, as shown in Table 4 below. The first case was where irregular predominant cracks were seen on the untreated expansive natural soil and treated soil samples blended with 5% and 15 % DE. The second case is at 10% and 20% DE blend with the expansive natural soil. The cracking mode observed was a uniform, regular radial shrinkage without significant surface cracking.

Table 4 shows the summary of the crack initiation stage (i.e., beginning of notable cracks/air entry point) and the completed dried stage (i.e., point at which the desiccated cracks reach their shrinkage potential limit). The crack initiation starts due to the reduction in the soil water content (i.e., increase of suction). Various research has indicated that the initial crack initiated at the soil commenced desaturating when the suction of the saturated soil subjected to desiccation attained the air entry value (AEV). Later, this phenomenon is followed by the gradual tensile stress development developed from the soil water and soil particle interactions through the continuum evaporation effect. The soil phase is also continuously changing dynamically due to the vaporization of the soil water. Through this continuum phenomenon, the soil matrix finally reaches its shrinkage potential at its completely dried state.

Table 4. Crack Propagation and End of Dried State of Untreated and Treated Samples

Soil Matrix	Crack Initiation State (START)	Complete Dried State (END)
ES + 0% DE		
ES + 5% DE		
ES + 10% DE		
ES + 15% DE		
ES + 20% DE		

5. CONCLUSIONS

The experimental results showed that diatomaceous earth could be used as an additive to reduce desiccation cracking of expansive soil. Furthermore, the results show that adding diatomaceous earth affects the desiccation cracking, which implies expansive soil's physical, mechanical, and chemical properties—the DE-expansive soil matrix with higher DE content spatial distribution in a desiccation cracking manner. Notably, the observed reduction in desiccation cracking at a mixture of 20% diatomaceous earth decreased the crack spatial distribution by 16%. Also, with an increase in diatomaceous content, the cracking connectivity at 10% and 20% diatomaceous earth soil matrix showed a maximum removal of crack connectivity. However, it was assumed that the water would be absorbed by adding diatomaceous earth, but the experimental results did not reflect that. This result was due to the high pore size distribution, resulting in a high evaporation rate.

6. RECOMMENDATIONS

This study recommends that further study is required to see the effectiveness of diatomaceous earth on the desiccation cracking of expansive soil. The influencing factors are categorized into microstructure and macro-structure-related parameters. The microstructure parameters include the cation exchange capacity, mineralogy, and microlevel particle arrangements. Macrostructure parameters are the tensile strength and shear strength of the soil.

7. ACKNOWLEDGMENTS

JST-JICA, SATREPS, grant number JPMJSA1807, Japan supported this work.

8. REFERENCES

- [1] Qi W., Wang C., Zhang Z., Huang M., and Xu J., Experimental Investigation on the Impact of Drying–Wetting Cycles on the Shrink–Swell Behavior of Clay Loam in Farmland. *Agriculture (Switzerland)*, Vol.12, Issue 2, 2022.
- [2] Li D., Yang B., Yang C., Zhang Z., and Hu M., Effects of salt content on desiccation cracks in the clay. *Environmental Earth Sciences*, Vol.80, Issue 19, 2021, pp. 1–13.
- [3] Tang C.S., Zhu C., Cheng Q., Zeng H., et al., desiccation cracking of soils: A review of investigation approaches, underlying mechanisms, and influencing factors. *Earth-Science Reviews*, Vol.216, Issue March 2021, pp. 103586.

- [4] Walke B., Seasonal Weather Assessment for Ethiopia. Issue July 2016, pp. 3.
- [5] Xie Y., Costa S., Zhou L., and Kandra H., Mitigation of desiccation cracks in clay using fiber and enzyme. *Bulletin of Engineering Geology and the Environment*, Vol.79, Issue 8, 2020, pp. 4429–4440.
- [6] Costa S., Kodikara J., Barbour S.L., and Fredlund D.G., Theoretical analysis of desiccation crack spacing of a thin, long soil layer. *Acta Geotechnica*, Vol.13, Issue 1, 2018, pp. 39–49.
- [7] Araujo A.G.D. De, Belfort N.T., Barbosa F.A.S., Silva T.C.R., et al., Expansive clay cracking behavior through digital image correlation. *E3S Web of Conferences*, Vol.195, 2020, pp. 4–8.
- [8] Nelson, J. D., and Miller, D.J., Chapter 2, Expansive soils, Problems and Practice in Foundation and Pavement Engineering. New York: John Wiley & Sons, 1992. pp.19-259
- [9] Xu Y., Yao X., Zhuang Y., Duan W., et al., The effects of fiber inclusion on the evolution of desiccation cracking in soil-cement. *Materials*, Vol.14, Issue 17, 2021, pp. 1–13.
- [10] KHALIFA A., Galaa A., and Mohamed M., Effect of Polypropylene Fibers Length and Content on Cracks Development in Clay Lining. *Journal of Al-Azhar University Engineering Sector*, Vol.17, Issue 62, 2022, pp. 65–82.
- [11] Barman D., and Dash S.K., Stabilization of expansive soils using chemical additives: A review. *Journal of Rock Mechanics and Geotechnical Engineering*, Vol.14, Issue 4, 2022, pp. 1319–1342.
- [12] Kumara G.H.A.J.J., Hayano K., and Ogiwara K., 290-295-1261-Kumara-Sept-2012. *Int. J. of GEOMATE*, Vol.3, Issue 1, 2012, pp. 290–297.
- [13] Shit P.K., Bhunia G.S., and Maiti R., Soil crack morphology analysis using image processing techniques. *Modeling Earth Systems and Environment*, Vol.1, Issue 4, 2015, pp. 1–7.
- [14] Tang C.S., Cui Y.J., Tang A.M., and Shi B., Experiment evidence on the temperature dependence of desiccation cracking behavior of clayey soils. *Engineering Geology*, Vol.114, Issue 3–4, 2010, pp. 261–266.
- [15] Cui Y.J., Tang C.S., Tang A.M., and Ta A.N., Investigation of soil desiccation cracking using an environmental chamber. *Rivista Italiana di Geotecnica*, Vol.48, Issue 1, 2014, pp. 9–20.
- [16] Wang J., Li X., Wen H., and Muhunthan B., Shrinkage cracking model for cementitiously stabilized layers for use in the mechanistic-empirical pavement design guide. *Transportation Geotechnics*, Vol.24, Issue December 2019, 2020, pp. 100386.
- [17] Zeng H., Tang C.S., Zhu C., Cheng Q., Lin Z. ze, and Shi B., Investigating Soil Desiccation Cracking Using an Infrared Thermal Imaging Technique. *Water Resources Research*, Vol.58, Issue 1, 2022, pp. 1–22.
- [18] Hu L.B., Hueckel T., Péron H., and Laloui L., Modeling evaporation, shrinkage and cracking of desiccating soils. *12th International Conference on Computer Methods and Advances in Geomechanics 2008*, Vol.2, Issue May 2014, 2008, pp. 1083–1090.
- [19] Abbaszadeh S., Houston S.L., and Zapata C.E., Effect of Desiccation Cracking on the Swell and Swell Pressure of Expansive Clay. *Geotechnical and Structural Engineering Congress 2016 - Proceedings of the Joint Geotechnical and Structural Engineering Congress 2016*, Issue July 2018, 2016, pp. 2054–2065.
- [20] Merlin O., Al Bitar A., Rivalland V., Béziat P., Ceschia E., and Dedieu G., An analytical model of evaporation efficiency for unsaturated soil surfaces with an arbitrary thickness. *Journal of Applied Meteorology and Climatology*, Vol.50, Issue 2, 2011, pp. 457–471.
- [21] Lu Y., Gu K., Zhang Y., Tang C., Shen Z., and Shi B., Impact of biochar on the desiccation cracking behavior of silty clay and its mechanisms. *Science of the Total Environment*, Vol.794, 2021.